A search for chameleon particles using a photon regeneration technique

A. S. Chou[1], W. Wester[2], A. Baumbaugh[2], H. R. Gustafson[3], Y. Irizarry-Valle[2], P. O. Mazur[2], J. H. Steffen[2], R. Tomlin[2], A. Upadhye[4], A. Weltman[5], X. Yang[2], and J. Yoo[2]

[1] *Center for Cosmology and Particle Physics, New York University, 4 Washington Place, New York, NY 10003*
[2] *Fermi National Accelerator Laboratory, PO Box 500, Batavia, IL 60510*
[3] *Department of Physics, University of Michigan, 450 Church St, Ann Arbor, MI 48109*
[4] *Kavli Institute for Cosmological Physics, University of Chicago, IL 60637*
[5] *Department of Applied Mathematics and Theoretical Physics,*
Centre for Mathematical Sciences, Cambridge CB2 0WA, United Kingdom
(Dated: June 15, 2008)

We report the first results from the GammeV search for chameleon particles, which may be created via photon-photon interactions within a strong magnetic field. The chameleons are assumed to have matter effects sufficiently strong that they reflect from all solid surfaces of the apparatus, thus evading detection in our previous search for weakly-interacting axion-like particles. We implement a novel technique to create and trap the reflective particles within a jar and to detect them later via their afterglow as they slowly convert back into photons. We constrain the coupling of chameleons to photons as a function of chameleon mass for a wide class of chameleon theories.

PACS numbers: 12.20.Fv, 14.70.Bh, 14.80.Mz, 95.36.+x

Introduction: Cosmological observations over the past decade have demonstrated with increasing significance the existence of a cosmic acceleration, usually attributed to a negative pressure substance known as "dark energy" [1, 2, 3]. A major effort is under way to discover the properties of dark energy, including its couplings to Standard Model fields. Such couplings can lead to Equivalence Principle violations [4], fifth forces [5], variations in Standard Model parameters such as the fine structure constant, and unexpected interactions between known particles. The chameleon mechanism, by which a matter coupling and a nonlinear self interaction conspire to give a field an environment-dependent effective mass, is particularly compelling from a cosmological standpoint [6, 7]. Chameleon fields can have small masses on cosmological scales, while acquiring large masses locally in order to evade fifth force searches [6, 7, 8, 9, 10, 11].

Chameleons may also couple to photons via terms such as $\phi F^{\mu\nu} F_{\mu\nu}$ and $\phi \tilde{F}^{\mu\nu} F_{\mu\nu}$, for scalars and pseudoscalars, respectively; here, $F_{\mu\nu}$ is the electromagnetic field strength tensor and $\tilde{F}_{\mu\nu}$ its dual. Such a coupling allows photons to oscillate into chameleons and back in the presence of an external magnetic field. The chameleon mechanism ensures that a chameleon with large couplings to matter will become massive inside typical laboratory materials. A chameleon with an energy less than the effective mass in a material will be completely reflected by that material, allowing chameleons to be trapped inside a "jar". Chameleons produced in the jar from photon oscillation will be confined until they regenerate photons, which emerge as an afterglow once the original photon source is turned off [12, 13, 14]. The GammeV experiment in its second incarnation is designed to search for such an afterglow. Note that the chameleon mechanism and the photon coupling are both necessary for this effect.

Chameleon phenomenology: A chameleon scalar field ϕ coupled to matter and photons has an action of the form

$$S = \int d^4x \left(-\frac{1}{2} \partial_\mu \phi \partial^\mu \phi - V(\phi) - \frac{e^{\phi/M_\gamma}}{4} F^{\mu\nu} F_{\mu\nu} \right.$$
$$\left. + \mathcal{L}_m (e^{2\phi/M_m} g_{\mu\nu}, \psi_m^i) \right) \quad (1)$$

where $g_{\mu\nu}$ is the metric, $V(\phi)$ is the chameleon potential, and $\mathcal{L}_m$ is the Lagrangian for matter; a pseudoscalar chameleon would instead have a chameleon-photon interaction $-\frac{\phi}{4M_\gamma} \tilde{F}^{\mu\nu} F_{\mu\nu}$. In principle, ϕ can couple differently to different matter particles. However, for simplicity, we consider a universal matter coupling $\beta_m = M_{Pl}/M_m$, where $M_{Pl} = 2.4 \times 10^{18}$ GeV is the reduced Planck mass. Theories with large extra dimensions allow matter couplings β_m much stronger than gravity, while an upper bound of $\beta_m \lesssim 10^{16}$ is obtained from particle colliders [15, 16], corresponding to $M_m > 100$ GeV. We allow for a different coupling to electromagnetism, $\beta_\gamma = M_{Pl}/M_\gamma$, through the electromagnetic field strength tensor $F_{\mu\nu}$. Curiously, this term resembles the dilaton-photon coupling $\sim e^{-2\phi} F^2$ in string theory.

The non-trivial couplings to matter and the electromagnetic field induce an effective potential

$$V_{eff}(\phi, \vec{x}) = V(\phi) + e^{\beta_m \phi/M_{Pl}} \rho_m(\vec{x}) + e^{\beta_\gamma \phi/M_{Pl}} \rho_\gamma(\vec{x}), \quad (2)$$

where we have defined the effective electromagnetic field density $\rho_\gamma = \frac{1}{2}(|\vec{B}^2| - |\vec{E}|^2)$ (for scalars) or $\rho_\gamma = \vec{E} \cdot \vec{B}$ (for pseudoscalars) rather than the energy density. The expectation value $\langle \phi \rangle$, the minimum of V_{eff}, depends on the density of both background matter and electromagnetic fields. Thus the effective mass of the chameleon, $m_{eff} \equiv \sqrt{d^2 V_{eff}/d\phi^2}$ evaluated at $\langle \phi \rangle$, will also depend on
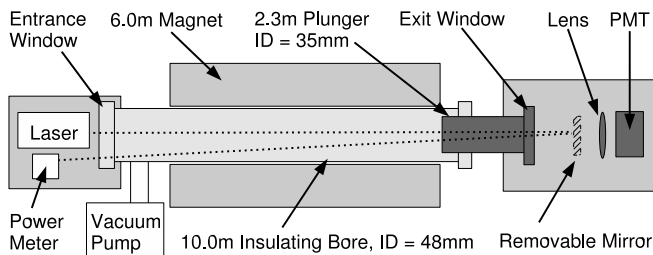
FIG. 1: The GammeV apparatus (not to scale). The chamber and the interior of the vacuum pump (total volume 0.049 m^3) are accessible to chameleon particles.

the environment. This dependence is crucial; the afterglow phenomenon requires that the particles be massive in the walls of the jar (to ensure containment) and that they remain sufficiently light inside the jar to allow coherent chameleon-photon oscillations. For a large range of potentials, the effective mass scales with ambient density as $m_{\rm eff}(\rho) \sim \rho^\alpha$, for α of order unity. For example, with a power law potential $V(\phi) \sim \phi^q$, where q is a real number, we find $0 < \alpha < 1$. This is true also for chameleon dark energy [17], $V(\phi) = \Lambda^4 \exp(\Lambda^n/\phi^n)$ with $\Lambda = 2.3$ meV, which is approximately $V(\phi) \approx \Lambda^4(1 + \Lambda^n/\phi^n)$ under laboratory conditions. Here, n is allowed to be any real number.

In order to provide model-independent constraints, we treat the effective chameleon mass inside the chamber as a free parameter. We note that for the power law potentials mentioned above, the chameleon coupling to the chamber walls contributes a quantity of order $1/R \sim 10^{-5}$ eV to the chameleon mass inside the chamber [10, 17], so that the total effective mass cannot be made lower than this. In regions near the walls of the apparatus, the larger effective masses ($> 10^{-3}$ eV) render the oscillations incoherent. The resulting regions of diminished regeneration efficiency are negligibly small compared to the total volume of the chamber.

GammeV apparatus: The GammeV apparatus, described in [18] and shown in Fig. 1, consists of a long cylindrical vacuum chamber inserted into the bore of a $B = 5$ T, $L = 6$ m Tevatron dipole magnet. The entrance and exit of the chamber are sealed with BK7 glass vacuum windows. A 20 Hz pulsed Nd:YAG laser [19] emits light of wavelength 532 nm (energy $\omega = 2.33$ eV) into the chamber at a rate of $F_\gamma \sim 10^{19}$ photons/sec.

Interactions with the magnetic field cause each photon to oscillate into a superposition of photon and chameleon states. This superposition can be measured in a quantum mechanical sense through collisions with the windows; chameleons bounce, while photons pass through. Repeated laser pulses build up the chameleon population inside the chamber. In order to populate the jar with chameleons, the laser is operated continuously for $\tau_{\rm pr} \approx 5$ h. After emerging through the exit window of the

chamber, the beam is reflected back through the chamber in order to increase the chameleon production efficiency and facilitate monitoring of the laser power.

During the afterglow phase of the experiment, the laser is turned off and a low noise PMT [19] placed at the exit window is uncovered. Chameleons interacting with the magnetic field oscillate back into photons, some of which escape to be detected by the PMT. Data are taken in two separate runs, with the polarization vector of the laser either aligned with or perpendicular to the magnetic field, to search for pseudoscalar as well as scalar chameleons.

Throughout the production and afterglow phases, a pressure $P \approx 10^{-7}$ Torr is maintained inside the vacuum chamber using a turbomolecular pump connected to a roughing pump. Because the low-mass chameleons are highly relativistic inside the chamber, the turbo pump simply acts as extra volume (0.026 m^3) for the chameleons. Our experiment can only test models in which the chameleon mass satisfies the conditions for coherent oscillation in the chamber, $m_{\rm eff} \ll m_{\rm osc} = \sqrt{4\pi\omega/L} = 9.8 \times 10^{-4}$ eV at $P_{\rm chamber} \approx 10^{-7}$ Torr, and reflection from the intake of the roughing pump, $m_{\rm eff} > \omega$ at $P_{\rm rough} = 1.9 \times 10^{-3}$ Torr. In the models with power law scaling discussed above, $m_{\rm eff} = m_0(P/P_{\rm rough})^\alpha \sim \rho^\alpha$, our constraints on β_γ are valid for $\alpha \gg 0.77$ and $\omega < m_0 < m_{\rm osc}(P_{\rm rough}/P_{\rm chamber})^\alpha$. In practice, we can constrain $\alpha > 0.79$ for scalars, and $\alpha > 0.86$ for pseudoscalars.

We test our apparatus by generating a diffuse low light level glow discharge within our upstream vacuum region and observing an increased PMT rate.

Expected signal: In terms of the coupling β_γ, and $m_{\rm eff}$ in the chamber, the chameleon production probability [20, 21, 22] per photon is

$$\mathcal{P}_{\rm pr} = \frac{4\beta_\gamma^2 B^2 \omega^2}{M_{\rm Pl}^2 m_{\rm eff}^4} \sin^2\left(\frac{m_{\rm eff}^2 L}{4\omega}\right). \qquad (3)$$

A particle that has just reflected from one of the chamber windows is in a pure chameleon state. Repeated bounces off of imperfectly aligned windows and the chamber walls cause chameleon momenta to become isotropic. As a chameleon passes through the magnetic field region, it oscillates between the photon and chameleon states. In the small mixing angle limit, the photon amplitude $\vec{\Psi}_\gamma$ due to this oscillation is given by

$$\left(-\frac{\partial^2}{\partial t^2} - k^2\right)\vec{\Psi}_\gamma = \frac{k\beta_\gamma B}{M_{\rm Pl}}\hat{k} \times (\hat{x} \times \hat{k})\Psi_\phi, \qquad (4)$$

where $\Psi_\phi \approx 1$ is the chameleon amplitude, $k \approx \omega$ is the momentum, and $\hat{k}$ and $\hat{x}$ are unit vectors in the direction of the particle momentum and the magnetic field, respectively. The chameleon decay rate corresponding to a particular direction (θ, φ) is $(|\vec{\Psi}_\gamma(\theta, \varphi)|^2 + \mathcal{P}_{\rm abs}(\theta, \varphi))/\Delta t(\theta)$ evaluated at the exit window, where θ is the direction with respect to the cylinder axis, $\mathcal{P}_{\rm abs}$ is the total probability of photon absorption in the chamber walls, and

$\Delta t(\theta) = \ell_{\text{tot}}/\cos(\theta)$ is the time required to traverse the chamber. We model a bounce from the chamber wall as a partial measurement in which the photon amplitude is attenuated by a factor of $f_{\text{ref}}^{1/2}$, where f_{ref} is the reflectivity. The mean decay rate Γ_{dec} per chameleon is found by averaging over θ and φ. Although the cylinder walls are not polished, a low absorptivity $1 - f_{\text{ref}} = 0.1$ is assumed in order to overpredict the coherent build-up of photon amplitude over multiple bounces. This overprediction of the decay rate results in a more conservative limit on the coupling constant. We obtain $\Gamma_{\text{dec}} = 9.0 \times 10^{-5}$ Hz for $\beta_\gamma = 10^{12}$, with $\Gamma_{\text{dec}} \propto \beta_\gamma^2$.

While the laser is on, new chameleons are produced at the rate of $F_\gamma \mathcal{P}_{\text{pr}}$ and decay at the rate of $N_\phi \Gamma_{\text{dec}}$. After a time τ_{pr} the laser is turned off, and the chamber contains $N_\phi^{(\text{max})} = F_\gamma \mathcal{P}_{\text{pr}} \Gamma_{\text{dec}}^{-1}(1 - e^{-\Gamma_{\text{dec}}\tau_{\text{pr}}})$ chameleon particles. For our apparatus, this saturates at 3.6×10^{12} for $\beta_\gamma \gtrsim 10^{12}$ and small m_{eff}. The afterglow photon rate is

$$F_{\text{aft}}(t) = \frac{f_{\text{vol}} f_{\text{esc}} \epsilon_{\text{det}} F_\gamma \mathcal{P}_{\text{pr}}^2 c}{\ell_{\text{tot}} \Gamma_{\text{dec}}} \left(1 - e^{-\Gamma_{\text{dec}}\tau_{\text{pr}}}\right) e^{-\Gamma_{\text{dec}}t}, \tag{5}$$

for $t \geq 0$, where $t = 0$ is the time at which the laser is turned off, and $f_{\text{vol}} = 0.40$ is the chamber volume as a fraction of the total accessible volume. The detector efficiency ϵ_{det} contains the 0.92 optical transport efficiency, as well as the 0.387 quantum efficiency and 0.7 collection efficiency of the PMT. A fraction $f_{\text{esc}} = 5.3 \times 10^{-7}$ of chameleons reach the exit window without colliding with the chamber walls, and virtually all of these reach the detector. While many chameleons that bounce from the walls may also produce photons which reach the detector (indeed, most of the photons that can reach the detector are on bouncing trajectories), such collisions result in a model-dependent chameleon-photon phase shift [17] which can affect the coherence of the oscillation on bouncing trajectories. Our goal here is to present results that, as much as is feasible, are independent of the chameleon model and can thus be applied more generally. We therefore consider only the direct light from non-bouncing trajectories in order to predict the minimum possible afterglow rate. Figure 2 shows the expected photon afterglow rate for several values of the photon-chameleon coupling β_γ. Non-observation of this underpredicted rate sets the most conservative limits. . However, we also note that the availability of other chameleon decay modes can weaken our constraints by allowing chameleons to decay quickly enough to escape detection. Furthermore, large chameleon self-interactions can lead to fragmentation and thermalization of chameleons, weakening our constraints. Such will be considered in a companion paper [23].

Results: After turning the laser off, we open the PMT box and remove the mirrors and filters that block the chamber from the PMT photocathode. Then, we replace the cover, turn the PMT on, and collect afterglow data
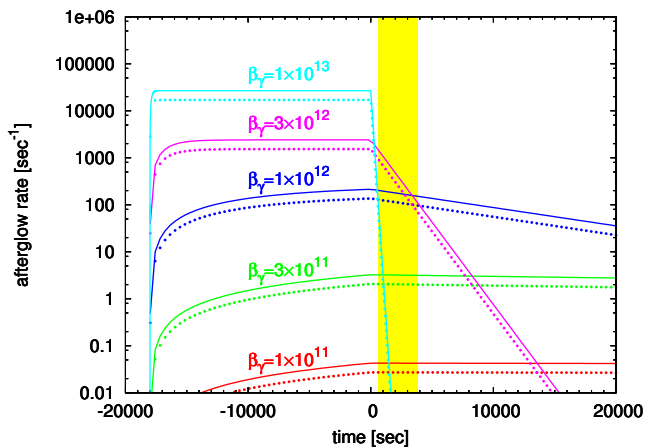

FIG. 2: Expected chameleon to photon conversion rate for various values of the coupling to photons β_γ. The solid curves are for chameleons with masses of 10^{-4} eV while the dotted curves are for 5×10^{-4} eV chameleons. Our observation time window for pseudoscalar chameleons is shown shaded in yellow; the corresponding time window for scalar chameleons is shifted to the right by about 700 sec.

for one hour. Table I shows relevant data for both of the data runs including: the total integration time during the filling stage, the total number of photons which passed through the chamber, a limit on the vacuum quality (which can affect the coherence length of the photon-chameleon oscillations), the length of the afterglow observation run, the time gap between filling the chamber and observing the afterglow, the mean afterglow rate, and the limits on β_γ for coherent oscillations.

In order to minimize the effects of systematic uncertainties, we compare the time-averaged expected afterglow signal to the mean signal observed by the PMT. The dominant uncertainty in our measurements of the chameleon afterglow rate is the systematic uncertainty in the PMT dark rate. We estimate this quantity, using data from [18], by averaging the count rate in each of 55 non-overlapping samples approximately an hour in length. The dark rate, computed by averaging the sample means, is 115 Hz, with a standard deviation of 12.0 Hz. The measured rates are well below the ~ 600 Hz maximum throughput of our data acquisition system. This systematic uncertainty is significantly larger than the statistical uncertainty in the individual sample means. Thus our 3σ upper bound on the mean afterglow rate is 36 Hz above the mean of the data for each run, after the background dark rate has been subtracted.

For each m_{eff} and β_γ we use (5) to compute the total number of excess photons predicted within the observation time window. Figure 3 shows the regions excluded by GammeV in the $(m_{\text{eff}}, \beta_\gamma)$ parameter space for scalar and pseudoscalar chameleon particles. At m_{eff} near $\sqrt{4\pi\omega/L} = 9.8 \times 10^{-4}$ eV, our exclusion region is limited by destructive interference in chameleon produc-

TABLE I: Summary of data for both configurations.

Configuration	Fill Time (s)	# photons	Vacuum (Torr)	Observation (s)	Offset (s)	Mean Rate (Hz)	excluded (low $m_{\rm eff}$)
Pseudoscalar	18324	2.39e23	2e-7	3602	319	123	$6.2e11 < \beta_\gamma < 1.0e13$
Scalar	19128	2.60e23	1e-7	3616	1006	101	$5.0e11 < \beta_\gamma < 6.4e12$
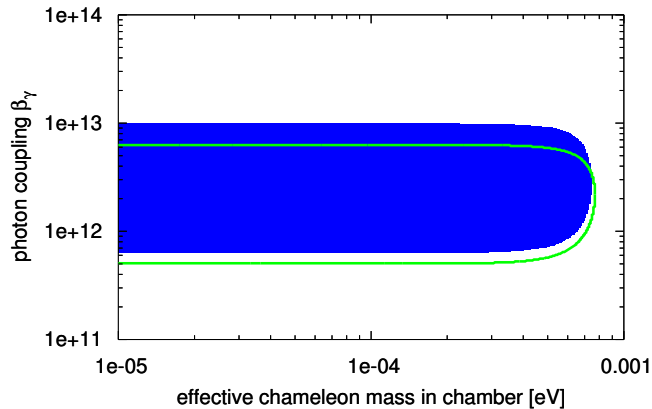
FIG. 3: Region excluded by GammeV to 3σ for pseudoscalar particles (solid blue region) and for scalar particles (region between green lines). Constraints worsen at $m_{\rm eff} \gtrsim 10^{-3}$ eV as photon-chameleon oscillation becomes incoherent. Chameleon interactions with the chamber walls typically prevent $m_{\rm eff}$ from dropping below $\sim 1/R \sim 10^{-5}$ eV.

tion. At higher $m_{\rm eff}$, a larger β_γ is needed to produce an equivalent non-bouncing minimum signal rate. However, for $\beta_\gamma \gtrsim 10^{13}$ our sensitivity diminishes because, as shown in Fig. 2, the chameleon decay time $\Gamma_{\rm dec}^{-1}$ in GammeV could be less than the few hundred seconds required to switch on the PMT. Our constraints could be extended to higher β_γ by more quickly switching on our detector, by understanding its systematics more thoroughly, and by making the chamber walls less reflective to reduce $\Gamma_{\rm dec}$. Finally, at low β_γ we are limited by our uncertainty in the PMT dark rate. At low $\Gamma_{\rm dec}$, (5) reduces to a constant rate $F_{\rm aft} \approx f_{\rm vol} f_{\rm esc} \epsilon_{\rm det} F_\gamma \mathcal{P}_{\rm pr}{}^2 c/\ell_{\rm tot}$, which, for $\beta_\gamma \lesssim 5\times10^{11}$, is below our detection threshold. In summary, GammeV has carried out the first search for chameleon afterglow, a unique signature of photon-coupled chameleons. Figure 3 presents conservative constraints in a model-independent manner.

[1] J. Frieman, M. Turner, and D. Huterer (2008), [arXiv:0803.0982 [astro-ph]].
[2] R. R. Caldwell, R. Dave, and P. Steinhardt, Phys. Rev. Lett. **80**, 1582 (1998).
[3] B. Ratra and P. J. E. Peebles, Phys. Rev. D **37**, 3406 (1988).
[4] C. Will, *Theory and Experiment in Gravitational Physics* (Basic Books/Perseus Group, New York, 1993).
[5] E. Fischbach and C. Talmadge, *The Search for Non-Newtonian Gravity* (Springer-Verlag, New York, 1999).
[6] J. Khoury and A. Weltman, Phys. Rev. Lett. **93** (2004), 171104.
[7] J. Khoury and A. Weltman, Phys. Rev. D **69** (2004), 044026.
[8] P. Brax, C. van de Bruck, A.-C. Davis, J. Khoury, and A. Weltman, Phys. Rev. D **70** (2004), 123518.
[9] S. S. Gubser and J. Khoury, Phys. Rev. D **70** (2004), 104001.
[10] A. Upadhye, S. S. Gubser, and J. Khoury, Phys. Rev. D **74** (2006), 104024.
[11] E. G. Adelberger et al., Phys. Rev. Lett. **98** (2007), 131104 [arXiv:hep-ph/0611223].
[12] The "particle trapped in a jar" technique was developed as part of the GammeV experiment, and independently realized in [13, 14].
[13] M. Ahlers, A. Lindner, A. Ringwald, L. Schrempp, and C. Weniger, Phys. Rev. D. **77** (2008), 015018 [arXiv:0710.1555 [hep-ph]].
[14] H. Gies, D. F. Mota, and D. J. Shaw, Phys. Rev. D. **77** (2008), 025016 [arXiv:0710.1556 [hep-ph]].
[15] D. F. Mota and D. J. Shaw, Phys. Rev. D. **75** (2007), 063501.
[16] D. F. Mota and D. J. Shaw, Phys. Rev. Lett. **97** (2006), 151102.
[17] P. Brax, C. van de Bruck, A. C. Davis, D. F. Mota, and D. J. Shaw, Phys. Rev. D **76** (2007), 085010 [arXiv:0707.2801 [hep-ph]].
[18] A. S. Chou and others [GammeV (T-969) Collaboration], Phys. Rev. Lett. **100** (2008), 080402 [arXiv:0710.3783 [hep-ex]].
[19] Laser: Continuum Surelite II I20. PMT: Hamamatsu H7422P-40.
[20] P. Sikivie, Phys. Rev. Lett. **51**, 1415 (1983), [Erratum-ibid. **52**, 695 (1984)].
[21] P. Sikivie, Phys. Rev. D. **32**, 2988 (1985), [Erratum-ibid. D **36**, 974 (1987)].
[22] G. Raffelt and L. Stodolsky, Phys. Rev. D. **37**, 1237 (1988).
[23] A. Chou et al. (2008), (in preparation).